

Material Classification Using Color and NIR Images

N. Salamati, C. Fredembach, S. Süsstrunk

School of Computer and Communication Sciences, Ecole Polytechnique Fédérale de Lausanne (EPFL), Lausanne, Switzerland

{neda.salamati, clement.fredembach, sabine.susstrunk}@epfl.ch

Abstract

Material classification is becoming more important in computer vision and digital photography applications, which require accurate classification of objects present in the imaged scene. This is a very challenging task because the sheer diversity of scene content and lighting conditions decreases the usefulness of many color- and texture-based features used in image classification. In this work, we investigate the potential offered by using information outside of the visible spectrum, specifically the near-infrared (NIR). The difference in the NIR images' intensities is not just due to the particular color of the material, but also absorption and reflectance characteristics of the colorant. This relative independency of NIR and color information makes NIR images a prime candidate for classification. The database, on which the training and testing were conducted, consists of textile, tile, linoleum and wood samples. To classify the materials, visible and NIR images were analyzed according to their lightness, texture, and color. The analysis results were the input to a classifier in form of feature vectors. The results show that our database is classified almost exactly. Comparing with visible-only features, wood and textile samples were better classified due to the additional information the NIR images provide.

KEYWORDS

Near-Infrared Imaging, Material Classification, Scene Analysis, Texture Analysis, Color Features.

INTRODUCTION

Computer vision, in recent years, has been extensively used in real world systems for a number of applications that rely on image segmentation, which requires accurate classification of object. Using a standard digital camera, there is almost no difference between two different materials with the same color under a given light source, i.e. a number of important object classes exhibit little or no differences in their RGB response, thus making them impossible to discriminate using standard methodologies. However, if one considers the electromagnetic spectrum beyond the range that the human visual system is sensitive to ($400 - 700\text{nm}$), visually similar samples may exhibit very different characteristics. In this work, we investigate the potential offered by using information outside of the visible spectrum, specifically near-infrared (NIR) images.

Near-infrared radiation lies just beyond the visible spectrum (wavelengths greater than 700nm). NIR images exhibit a few distinct effects [1]; most of the pigments and dyes used for material colorization are somewhat transparent to NIR [2], so different NIR intensity in the NIR images gives the information pertinent to material classes rather than the color of that object. In NIR im-

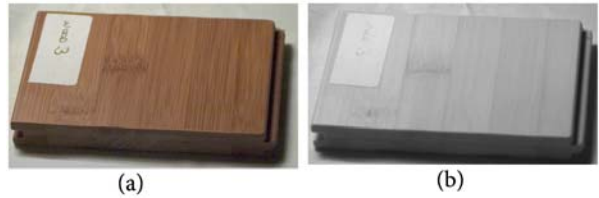


Figure 1: A typical photograph from a wood sample in the a) visible b) NIR part of the spectrum. The colorant is transparent to the NIR and intrinsic texture is observed.

ages, the observed surface texture appears more intrinsic, hence studying it leads to more accurate results than only using visible images (see Fig. 1 for illustration).

In this paper we propose a material classification method using sample's image in the visible (RGB) and in the NIR (a single channel image) part of the spectrum.

Image classification using NIR information has been widely used in remote sensing. As opposed to our method where, the image is single channel in the NIR range, in remote sensing it is multi-spectral and contains the spectral information of the samples being observed in the visible and NIR part of the spectrum. The reflectance spectrum of a material serves as a unique signature for the material [3].

Other scientific applications of near-infrared for material classification focus on near-infrared spectroscopy (NIRS), wherein a small part of the sample is placed inside the spectroscope and the near-infrared light is employed to measure spectral characteristics of test objects [4]. NIRS is a nondestructive analytical technique for studying interactions between incident light and a material's surface. However, in our method the classification is done by the features extracted from the whole sample and in addition to the NIR information, color and texture information are also used. NIRS has been found to be a useful technique to characterize materials such as textile, polymer and wood products [4].

Image-based classification methods, on the other hand, have focused on the extraction of color, shape and various texture analysis. Color is a basic feature used to extract a number of different information from an image [5]. Texture information can also be extracted to facilitate material classification [6,7].

In this paper, we classify four different types of materials: textile, tile, wood, and linoleum. All the images were taken under controlled viewpoint and illumination conditions and their analysis was conducted in both the frequency and spatial domain. Image features include the relation between materials' intensity in the NIR and luma in the color images, texture (in the frequency domain), and color.

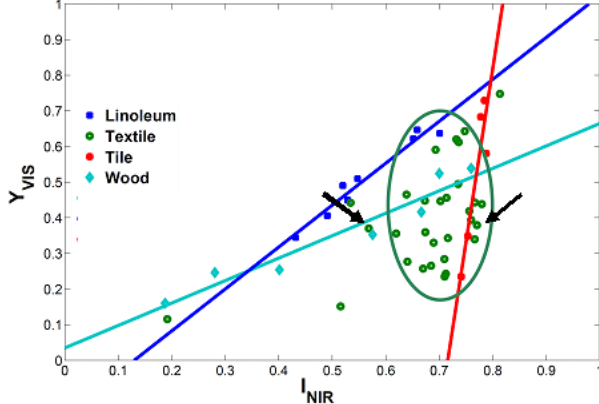


Figure 2: Intensity in NIR versus luma in color images. In wood, tile and linoleum, linear behavior is observed while for textile a two dimensional Gaussian can be fitted. The solid lines represent the respective linear regressions and the ellipse is the projection of the 2D Gaussian. The two textile samples, specified by black arrows, have roughly the same luma but different NIR intensities.

After extracting the relevant features and calculating the corresponding feature values, the materials were classified according to a simple probability function. The results show that our limited database is classified almost exactly, and comparisons with visible-only features show that adding NIR information yield a substantial increase in the classification rates.

CLASSIFICATION FRAMEWORK

To classify the materials in the database, visible and NIR images were analyzed according to their lightness, texture, and color. The database consists of 51 wood, tile, textile and linoleum samples. The analysis results are the input to a classifier in form of feature vectors to calculate the probability of that sample to belong to a material category.

Image Analysis

The images analysis comprises three steps. First, a comparison is made between the samples' luma in the visible and NIR images, followed by a texture and color analysis.

Luma Analysis

Since the pigments used for colorizing materials are somewhat transparent to NIR [2], we start by comparing the luma of the visible image to the NIR intensity.

The YC_bC_r color space separates chroma information of an image from luma information. Luma (Y), which is the weighted sum of the non-linear RGB components after gamma correction, is determined by:

$$Y = 0.2989R' + 0.5870G' + 0.1140B' \quad (1)$$

Where R' , G' and B' are the normalized sRGB values.

Y in color images (Y_{VIS}) and intensity in NIR images (I_{NIR}) [1] are calculated for all samples. Fig. 2 plots I_{NIR} versus Y_{VIS} for all samples in the database. Note that the intensity in the NIR images is always higher than luma in the visible images. In

addition, samples in each of the wood, tile, and linoleum classes form a line, which can be represented by a linear regression. The regression lines show high correlation coefficient values of $r^2 = 0.93$, 0.86 , and 0.93 , for tile, wood, and linoleum, respectively.

The I_{NIR} for almost all textile samples, however, lies in the narrow range between 0.6 and 0.8 . Y_{VIS} , on the other hand, lies in a broader range. As illustrated in Fig. 2, the relation between textile intensity in NIR and luma in color images can be modeled by a two dimensional Gaussian, whose mean and variance are:

$$\mu_v = 0.4 \quad \mu_h = 0.7 \quad \sigma_v = 0.13 \quad \sigma_h = 0.07 \quad (2)$$

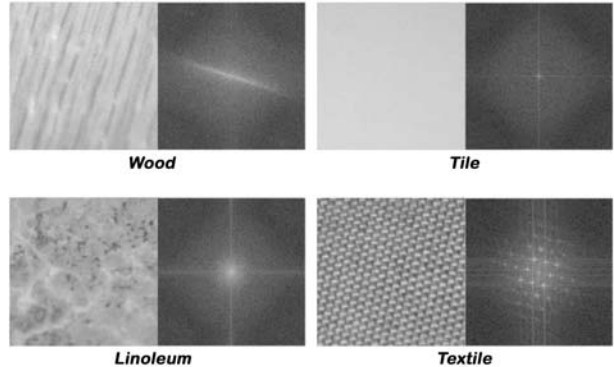


Figure 3: Samples in the spatial (left) and frequency (right) domain. The frequency spectra shows energy patterns that are characteristic of the materials' surfaces. A line can be observed in the wood sample due to the existing parallel lines on the surface. The peaks for the textile sample are due to the nature of the woven fabric. In tile and linoleum there exists high energy in low frequencies.

Texture Analysis

Images of real objects often do not exhibit regions of uniform lightness. For instance, the image of a wooden surface contains variations in intensities that form certain repeated patterns due to its specific surface characteristics. Figure 3 displays samples from different materials in the spatial and corresponding frequency domain. Due to the nature of woven fabric, where the surface is formed by a series of straight parallel lines crossing each other, a number of peaks in certain frequency bands can be witnessed. The naturally existing parallel lines on the wood surface result in the formation of a line at a specific angle in the frequency domain. Tiles' smooth surface leads to most energy being located in low frequencies.

To analyze these texture characteristics, we use here filters adapted from Ginsburg [8], namely ring and rectangular filters. Ring filters are used for analyzing the energy in certain frequency bands, while rectangular filters are employed for orientation detection. Ring filters $H_{ring}^{(i)}$ are Gaussian functions and defined according to:

$$H_{ring}^{(i)}(w_1, w_2) = \exp \left(- \left(\frac{(r - \mu_i)}{\sigma_i} \right)^2 \right) \quad (3)$$

$$r = \sqrt{w_1^2 + w_2^2} \quad (4)$$

where w_1, w_2 are spatial frequencies in the spatial domain. μ_i and σ_i are parameters determining the center frequency and the bandwidth of each ring filter, respectively. The filters are nondirectional (See Fig. 4). In this paper, 13 ring filters have empirically been chosen and applied.

The other set of filters are rectangular filters H_{rect} that are constructed according to:

$$w_1 - \tan(\theta \times w_2) - \frac{0.1}{2 \times \cos \theta} \leq H_{rect} \leq w_1 - \tan(\theta \times w_2) + \frac{0.1}{2 \times \cos \theta} \quad (5)$$

where θ varies from 0 to π , i.e., the rectangular filter is rotated and the energy is calculated at each angle. The width of the filters is constant and empirically chosen to be 0.2.

Different materials can be colorized in such way that their patterns give the same features as other materials in the texture analysis. Knowing that some colorants used in printed material are usually transparent to NIR, using NIR images for texture analysis avoids such problems.

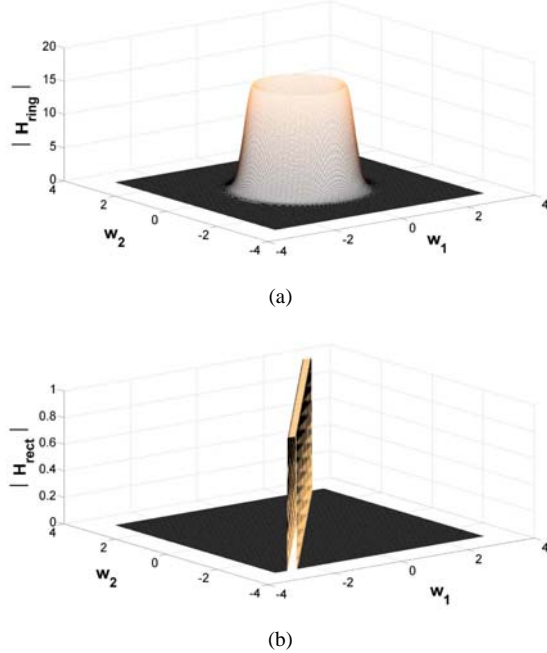


Figure 4: Representations of one of the a) ring and b) rectangular filters in the frequency domain. The height of the surface above the w_1, w_2 plane and the color level values represent the filter's amplitude.

Color Analysis

The process of colorizing a manufactured object is complex and varies according to the material; the colorants themselves are also diverse [2]. Although different colorants may look identical in color images, they have different responses in NIR images. Therefore, color information of the samples and the

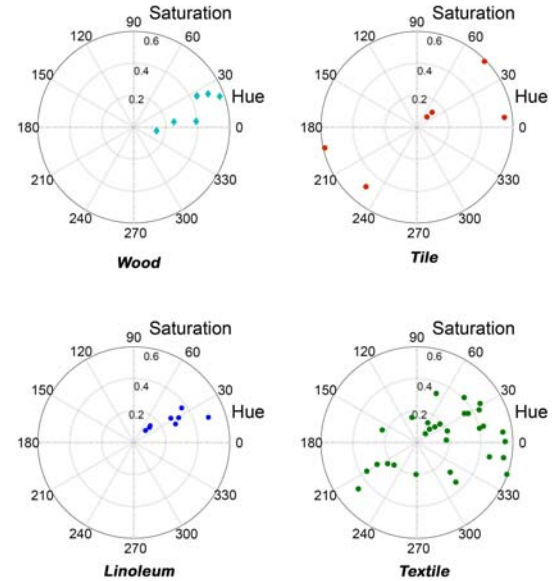


Figure 5: Hue versus saturation in color images. In wood samples, hue varies within a narrow angle, however, they have a wide range of saturation. To be expected tile and textile samples cover almost all hue and saturation values. The linoleum samples in our database are also within a narrow hue range and are not very saturated. However, this is due to our limited sample selection.

corresponding NIR intensities can be an important cue. We employ the hue, saturation and luminance (HSL) space [11], used in color image processing. Although almost all colors of the visible spectrum can be produced by merging primaries, the process of colorizing different material makes each class of material capable of having only a limited gamut (i.e., the set of possible colors within a material) of the visible spectrum (see Fig. 5 for illustration). Samples that have the same luma in color images may or may not have the same NIR intensity (see Fig. 2). The two textile samples, indicated by black arrows in Fig. 2 have roughly the same luma but different NIR intensities. The hue values in these two samples are different (see Fig. 6), i.e., the difference in NIR intensity for the same material can be related to the difference in hue. Hence, analyzing the gamut of each existing material, obtained using hue and saturation from the color image and the intensity from the NIR image of each sample may lead us to a better classification of material.

To do so, the RGB values of each sample are first converted into HSL and the luminance is replaced by the intensity of the NIR image. A 3-D convex hull algorithm was applied to determine the position and the volume of the gamut for each material class.

From Features to Classification

In this section, we explain how to obtain feature vectors and classify materials from the acquired features. First, features are selected and then the probability of a sample to belong to a material class is calculated. We explain how to calculate the probability pertinent to each analysis.

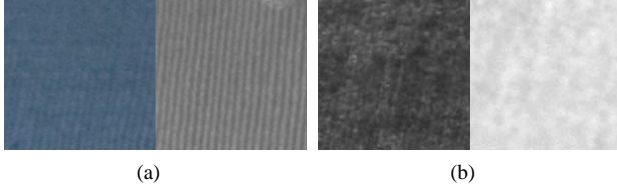


Figure 6: Images of two textile samples with the same luma in the visible part of the spectrum but different NIR intensity. The difference in intensity in the NIR images can be related to the difference in their hue.

Feature Extraction

From each analysis, features are selected to quantify material characteristics. The choice of appropriate descriptive parameters will significantly influence the effectiveness of the classification. Intensity in NIR and luma in color images are taken to be feature values T_1 and T_2 .

$$T_1 = I_{NIR} \quad T_2 = Y_{VIS} \quad (6)$$

For texture, we normalized the energy existing in different ring filters.

$$\bar{E}_{ring}^{(i)} = \frac{E_{ring}^{(i)}}{\max_{i=1\dots 13} (E_{ring}^{(i)})} \quad (7)$$

$$E_{ring}^{(i)} = \|F_I(w_1, w_2) \times H_{ring}^{(i)}\|^2 \quad (8)$$

Where \bar{E}_{ring} is the normalized energy, $F_I(w_1, w_2)$ is the Fourier transform of the image I , and $\|\cdot\|$ denotes the Frobenius norm (see Fig. 7 for a representative sample from each material category). For all the non-textile samples, the larger the diameter of the ring filter, the less the spectral energy in the corresponding ring filtered image, i.e., most of the energy lies in the low frequency part of the spectrum. For the textile samples, however, the existing peaks in the high frequencies due to the nature of the woven fabric will result in an increase of the energy in the ring filtered images incorporating those peaks. Hence, the filtered image for which the energy is maximum can be taken into consideration as a feature value, which we call T_3 . For simplicity, this feature value can be reduced to a binary value:

$$T_3 = \begin{cases} 0 & \text{if } \operatorname{argmax}_{i=1\dots 13} (\bar{E}_{ring}^{(i)}) = 1 \\ 1 & \text{otherwise} \end{cases} \quad (9)$$

Fig. 8 displays the energy existing in different rectangular filters for all angles between 0 and π , one degree interval, for a random sample from each material category. In the smooth samples, like tiles, the energy is constant at all angles, for oriented texture samples (such as wood), an energy peak is observed at a specific angle. For textile samples, due to the existence of peaks in the frequency domain, more than one peak of energy is observed at some specific angles.

The energy peak at a certain angle is detected when its distance to the energy of surrounding angles is more than a certain threshold. The considered threshold δ will reduce the sensitivity

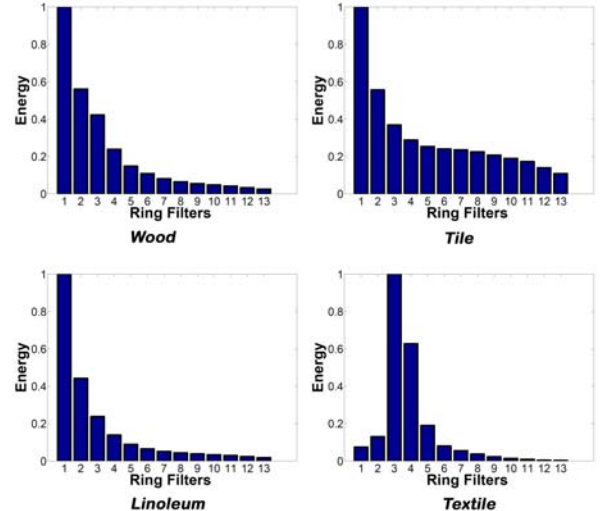


Figure 7: Relative energy $\bar{E}_{ring}^{(i)}$ in all 13 ring filtered images for a random sample in each class. The corresponding T_3 value for each sample is: [0,0,0,1].

of the algorithm to noise, thus it is taken as the variance of that signal,

$$\delta_x = \frac{\sum_{i=1}^{180} (E_x^{(i)} - \bar{E}_x^{(i)})^2}{180} \quad (10)$$

$$E_x^{(i)} = \|F_I(w_1, w_2) \times H_{rect}^{(i)}\|^2 \quad (11)$$

where $E_x^{(i)}$ is the energy existing in the i^{th} rectangular filtered image and $\bar{E}_x^{(i)}$ is the average of the energy over all rectangular filters. As a result, the existence of one or more peaks at an angle is used as the feature value T_4 .

$$T_4 = \begin{cases} 0 & \text{if } N_p = 0 \\ 1 & \text{if } N_p = 1 \\ 2 & \text{otherwise} \end{cases} \quad (12)$$

Where N_p is the number of detected peaks.

The fifth feature vector contains the hue, saturation, and NIR intensity coordinates.

$$T_5 = \{Hue, Saturation, I_{NIR}\} \quad (13)$$

Luma Related Probability

As seen in section 2, wood, tile, and linoleum have Y_{NIR} varying linearly with Y_{VIS} . This behavior is easily modeled by linear regression:

$$\hat{Y}_{ij} = X_{ij} \hat{\beta}_i \quad (14)$$

where $\hat{\beta}_i = (X_i^T X_i)^{-1} X_i^T \hat{Y}_i$, and $\hat{Y}_i = X_i (X_i^T X_i)^{-1} X_i^T Y_i$. Y_i is the luma of the visible images and X_i contains the corresponding intensity in NIR images.

From this, the vector of residuals can be defined as [12]:

$$\hat{e}_i = Y_i - \hat{Y}_i \quad (15)$$

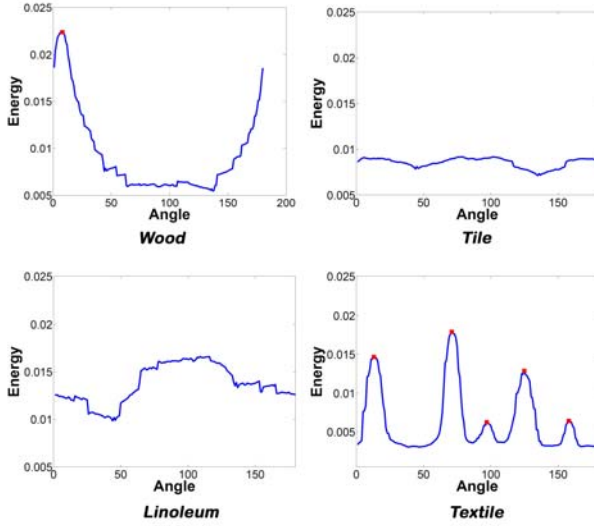


Figure 8: The energy in the rectangle filter from 0 to 180 degrees for a random sample in each class. The detected peaks are marked by red circles. The corresponding T_4 value for each sample is: [1,0,0, 2].

By studentizing the residuals [12], we are able to determine the probability of sample x belonging to tile, wood, or linoleum. For each line, the variance of the residuals for all samples can be calculated under a certain confidence level α_i . Variance of residual of each sample defines the distance from the regression line that shows how much further from the regression line a new samples in that material class can fall. In other word, we can be $\alpha_i\%$ sure that all samples in the material class fall in the area around the regression line that has been defined by the maximum variance of residual. Moreover, we are $(1 - \alpha_i)\%$ sure that our target sample belongs to the line representing the class when that sample is located outside of that area. The probability for any new sample to belong to each class can be calculated by the maximum confidence interval that makes an area so that the target sample is outside of the area:

$$P_L((x \in A_{i=1\dots 3}) | T_1, T_2) = 1 - \alpha \quad (16)$$

where α is the maximum confidence interval forming an area to which sample x doesn't belong, $A = \{A_i | i = 1 \dots 3\}$ represent tile, wood, and linoleum, respectively. The residual variance is calculated within the confidence interval of α , thus $1 - \alpha$ is the probability that the sample belongs to that class (see Fig. 8 for illustration).

For the textile class, we model the relationship between I_{NIR} and Y_{VIS} as a 2D Gaussian function. $P(textile | T_1, T_2)$ is thus given by:

$$P_L((x \in A_4) | T_1, T_2) = \frac{1}{2\pi\sigma_v\sigma_h} e^{-\frac{1}{2}\left(\frac{T_1^2 - \mu_v}{\sigma_v} + \frac{T_2^2 - \mu_h}{\sigma_h}\right)} \quad (17)$$

where σ_v and σ_h are the variance and μ_v and μ_h are the mean of the two Gaussians with respect to the color and NIR images. The values of σ and μ were given in section 2. We are, however,

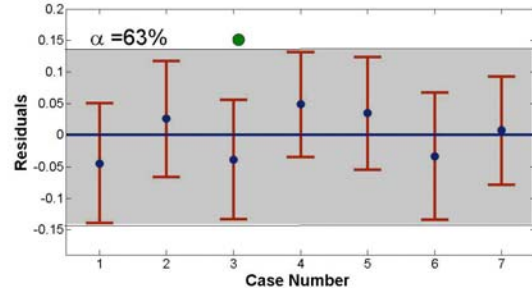


Figure 9: The residuals of the wood samples within 63% confidence interval. The black line is the regression line representing the correlation of the wood samples in the database. The area in which we are 63% confident that samples are wood is shaded gray. Thus the probability of the target sample (green point) to be wood is 37%.

T_3	T_4	Textile	Tile	Wood	Linoleum
1	0	4/30	0	0	0
1	1	6/30	0	0	0
1	2	13/30	0	0	0
0	0	3/30	6/6	7/8	0
0	1	4/30	0	1/8	7/7
0	2	0	0	0	0

Table 1: $P(T_3, T_4 | A_i)$ in the database.

interested in the probability of a sample belonging to one class (A_i) but not the other ($x \neq A_{j \neq i}$):

$$P_L((x \in A_i \cap (x \neq A_{j \neq i})) | T_1, T_2) = \frac{P(x \in A_i | T_1, T_2) \times P(A_i)}{\sum_{i=1}^n (P(T_1, T_2 | A_i) \times P(A_i))} \quad (18)$$

where

$$P(A_i) = \frac{N_i}{N_T} \quad (19)$$

and N_i is the number of samples existing in the i^{th} material in the database and N_T is the total number of samples in the database.

Texture Related Probability

In order to calculate the probability of a sample to belong to a material category, knowing T_3, T_4 , the Bayes theorem is used.

$$P_T((x \in A_i) | T_3, T_4) = \frac{P(T_3, T_4 | A_i) \times P(A_i)}{\sum_{i=1}^n (P(T_3, T_4 | A_i) \times P(A_i))} \quad (20)$$

$P(T_3, T_4 | A_i)$ can be defined as number of cases favorable for the feature vector $[T_3, T_4]$, over the number of total samples in material A_i . We calculate this probability for each feature vector, i.e., the probability of each sample of a certain material to have a certain feature value $[T_3, T_4]$ (see Table 1).

Color Related Probability

Knowing the position of a new sample in H, S and I_{NIR} color space (T_5) as well as the gamut for each material class, we can conclude that if (T_5) exists in the gamut of material A_i , then that

sample will belong to the class A_i . Therefore, the following statement can be used to specify the probability of a sample to belong to the material class A_i :

$$P_C(x \in A_i) = \begin{cases} \frac{1}{n} & \text{if } T_5 \in \text{Gamut}_{A_i} \\ 0 & \text{if } T_5 \notin \text{Gamut}_{A_i} \end{cases} \quad (21)$$

where n is the number of material classes whose gamuts intersect at the position of T_5 .

Final Probability Estimation

We assume that the probabilities resulting from luma and color analysis is independent from texture analysis, so for that neither luma nor color of a material impact the surface characteristics of that material.

To investigate the dependency of color and luma analysis, we should mention the fact that three attributes of color in HSL are decorrelated [13], i.e., knowing the relation between luma and NIR intensity does not give us any information about the relation between hue, saturation and NIR intensity.

Thus the corresponding probabilities are independent. The final probability for each sample can be calculated by multiplying the probabilities given from each analysis:

$$P(x \in A_i | T_1, \dots, T_5) = P_L \cap P_T \cap P_C = P_L \times P_T \times P_C \quad (22)$$

$P(x \in A_i | T_1, \dots, T_5)$ represents the probability of a sample x to belong to a material category A_i according to feature values T_1 to T_5 .

EXPERIMENT

All samples were photographed in the visible and in the near-infrared range of the spectrum in a controlled environment. The camera we used in these experiments is a Canon EOS 300D and the light source was incandescent. The photography operation followed the same procedures for the two types of photographs taken from the samples. The database on which the training and testing were conducted consists of 30 textile, 5 tile, 8 linoleum and 7 wood samples.

In order to determine how accurately this learning algorithm will be able to predict a new sample's material, leave-one-out cross validation has been applied. When using the leave-one-out method, the learning algorithm is trained multiple times, using all but one of the data points and then testing the removed data point and calculating the probability of that sample to belong to each class.

For the entire database, the feature vectors are formed and the probability of each sample having a certain feature vector, given the material, is calculated. The probability of each sample belonging to each material given the feature vector is calculated according to Eq. 22 for each left-out sample.

The algorithm was applied to all the samples in our dataset and the probability of each left-out sample belonging to each material category was calculated. The higher the probability, the better we could come to the conclusion that the sample belongs to a certain category.

To assess the usefulness of NIR information, the classification was performed using visible features only (results in Table 2) as well as using visible and NIR features (results in Table 3). We see

	Textile	Tile	Linoleum	Wood
Textile	25/30	0	0	5/30
Tile	0	6/6	0	0
Linoleum	0	7/8	0	1/8
Wood	0	0	1/7	6/7

Table 2: The confusion matrix using just visible information

	Textile	Tile	Linoleum	Wood
Textile	29/30	0	0	1/30
Tile	0	6/6	0	0
Linoleum	0	0	8/8	0
Wood	0	0	0	7/7

Table 3: The confusion matrix using both visible and NIR information.

that the additional NIR information makes the proposed classification more accurate. The wood and textile samples were classified better due to transparency of most of the colorants to the NIR light in the sample; as a result the NIR images provide more effective data.

CONCLUSION

In this paper, a database consisting of four different types of materials was used. The images of all samples in the database were taken in the NIR and visible part of the spectrum. The analysis of luma, intensity, and color information of the two images revealed that some of the pigments used to colorize some materials are transparent to NIR. The relation between the visible and NIR information yield an improvement in image-based machine classification. The materials were more accurately classified when NIR information was present. The result and framework are suited for the samples in our data base and they may not generalize to more material classes. Our future work will focus on extending the database by including more material classes such as plastic and metal, as well as incorporating other texture analysis methods that are more scale invariant.

Acknowledgment

The work presented in this paper was supported by the Swiss National Science Foundation under grant number 200021-124796/1.

References

- [1] C. Fredembach and S. Süsstrunk. Colouring the Near-Infrared. In *Proceeding of IS&T 16th Color Imaging Conference*. Portland, 2008
- [2] A. A. Tracton. *Coating Technology Handbook*. 3rd ed., CRC Press, 2006.
- [3] R. A. Schowengerdt. *Remote sensing: models and methods for image processing*. Third edition, Academic Press, 2007.
- [4] D.A. Burns and E.W. Ciurczak. *Handbook of near-infrared analysis*. Marcel Dekker Inc., 2001.
- [5] S. B. Park, J. W. Lee, and S. K. Kim. Content-based image classification using a neural network. *Pattern Recognition Letters*. vol. 25, pp. 287-300, 2004.
- [6] A. Drimbarean and P.F. Whelan. Experiment in Color Texture Analysis. *Pattern Recognition Letters*. vol. 22, pp. 1161-1167, 2001.
- [7] M. Petrou and M. Mirmehdi. Segmentation of Color Textures. *IEEE*

- Trans. on Pattern Analysis and Machine Intelligence.* vol. 22(2), pp. 142-159, 2000.
- [8] T. Randen and J. H. Husoy. Filtering for Texture Classification: A Comparative Study. *IEEE Trans. on Pattern Analysis and Machine Intelligence.* vol. 21(4), pp. 291-309, 1999.
 - [9] P. Lambert and T. Carron. Symbolic Fusion of Luminance-Hue-Chroma Features for Region Segmentation. *The journal of the pattern recognition society.* vol. 32, pp. 1857-1872, 1999.
 - [10] J. Richard Aspland. *Textile Dyeing and Coloration*. American Association of Textile Chemists and Colorists., 1997.
 - [11] X. Zhang, C. Broun, R. Mersereau, and M. Clements. Automatic speechreading with applications to human-computer interfaces. *iEURASIP Journal on Applied Signal Processing.* vol. 11, pp. 12281247, 2002.
 - [12] R. D. Cook, S. Weisberg. *Residuals and Influence in Regression*. Chapman and Hall, 1982.
 - [13] A. Reed and B. Hannigan. Adaptive Color Watermarking. in *Proceeding of SPIE Electronic Imaging.* vol. 4675, San Jose, CA, USA, 2002

Author Biography

Neda Salamati received her BSc and MSc in Chemical (Textile) Engineering from Tehran Polytechnic University. Since 2008, she is a Research Assistant in Color Imaging, pursuing a PhD degree in the Audio-visual Communications Laboratory, EPFL.